COUNTERMEASURES AGAINST SEA LEVEL RISE USING SEAWALL WITH MULTIPLE WAVE OVERTOPPING MEASURES (SMO)

Tatsuki Suzuki, Pacific Consultants Co., LTD, tatsuki.suzuki@tk.pacific.co.jp
Kojiro Suzuki, Port and Airport Research Institute, suzuki_k@p.mpat.go.jp

INTRODUCTION

In Japan, there are many seawalls where it is difficult to raise the crown height from the viewpoint of obstacle limitation surfaces at airports and deteriorated landscapes. As a measure to reduce the wave overtopping rate and lower the crest height, a *s*eawall with *m*ultiple wave *o*vertopping measures (***SMO***), which combines a Recurved Parapet (R.P.), a Double Parapet (D.P.), and a Permeable Layer (P.L.). Figure 1 shows a practical application of ***SMO***. ***SMO*** creates a beautiful coastal landscape and is used as a place of relaxation for the neighborhood residents. However, the effect of ***SMO*** on reducing wave overtopping rate has not been systematically investigated. Therefore, its applicability to the anticipated increase in wave overtopping rate due to sea level rise is also unclear.

In this study, we evaluated the wave overtopping suppression effect of ***SMO*** using hydraulic model experiments and numerical simulations.Furthermore, the effect of sea level rise on reducing wave overtopping of ***SMO*** was verified by numerical simulation.

HYDRAULIC MODEL TEST AND CALCULATIONS

We conducted hydraulic model experiments on a 1/16-scale model of the seawall of N-Airport (Figure 2). The experiment was conducted at five tide levels. That is, H.H.W.L. and +0.5m, +1.1m, +1.4m, +1.7m. Plus 0.5m and +1.1m correspond to the tide level when the temperature increases by 2K or 4K. Significant wave height and wave period in front of the seawall was 4.1m and 14.7s(field scale). Figure 3 shows the experimental results for a vertical seawall (existing seawall) and ***SMO*** with sea level rise (S.L.R.) =1.1m. In the case of the vertical wall, severe wave overtopping occurred. In contrast, in the case of SMO, the amount of wave overtopping was greatly reduced. Figure-4 shows the relationship between sea level rise and wave overtopping rate. When sea level rises, the wave overtopping rate of vertical seawall greatly exceeds the tolerable wave overtopping rate. Here, the tolerable overtopping rate of seawalls in Japan is 0.02 m^3/s/m. ***SMO*** tends to reduce the wave overtopping rate by about 2 orders of magnitude compared to the vertical seawall. The wave overtopping rate of ***SMO*** is below (almost equal to) the tolerable overtopping rate even at S.L.R. = 1.4 m. These results confirm that the ***SMO*** is effective in reducing wave overtopping rate.

We reproduced these experiments by using CADMAS-SURF/3D (**CS**) based on the VOF method. Numerical simulation results showed good reproducibility. Therefore, the following studies was conducted by using the **CS** numerical calculations.

COMPARISON OF VARIOUS WAVE OVERTOPPING MEASURES

Figure-5 shows the cross-sections of the vertical wall

Figure 1 - Example of ***SMO*** (Kanagawa, Japan)

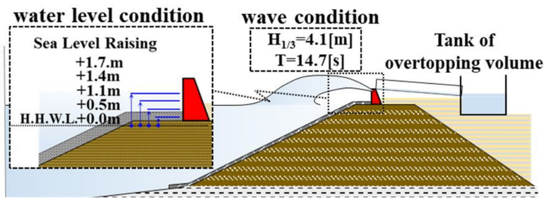

Figure 2 - Cross section of hydraulic model experiment

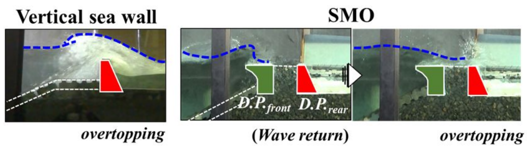

Figure 3 - Wave overtopping situation by the experiments

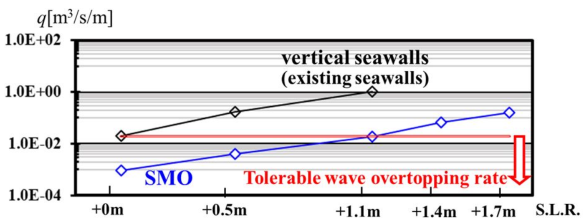

Figure 4 - Experimental results of wave overtopping rate considering sea level rise

(existing wall) and improved seawalls (various wave overtopping measures, R.W., D.P., and P.L.) modeled in **CS**. Figure 6 shows the wave overtopping situation for four different seawall cross sections. Figure 7 shows the wave overtopping rate of the improved seawalls.

First, a large wave overtopping occurred in the vertical wall. R.W. intends to reduce waqve overtopping by changing the direction of motion of upward moving water masses to the offshore side. However, when the water level is relatively high, the wave return effect and wave overtopping reduction effect are small. In the D.P., water overtopping occurs first at the D.P.$_{front}$, followed by wave caused wave overtopping of the D.P.$_{front}$, and the water mass in the ponding area overtopped the D.P.$_{rear}$.

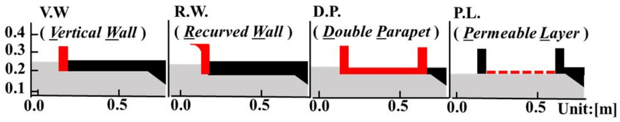

Figure 5 - Vertical wall and improved seawalls

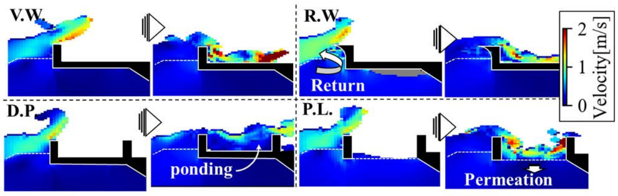

Figure 6 - Wave overtopping situation of vertical wall and improved seawalls (S.L.R.+0.0m)

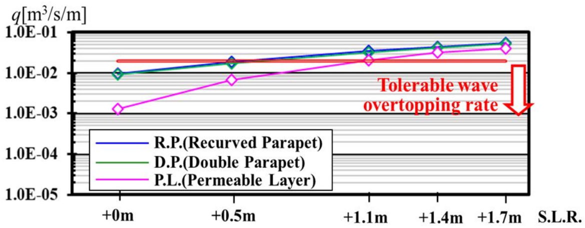

Figure 7 - Wave overtopping rate changes of improved seawalls due to S.L.R.

In the case of P.L., the ponding at parapet-to-parapet in D.P. returns to the offshore side through the permeable layer, which reduces the wave overtopping rate compared to the other two types.
However, when the water level between the parapets is high and S.L.R. = 1.1m, where the wave overtopping rate from the D.P.front is high, the wave overtopping rate reduction effect becomes smaller because the drainage effect from the permeable layer becomes smaller.

EVALUATION OF WAVE OVERTOPPING FOR *SMO*

Figure-8 shows the cross-sections of the ***SMO***s for which calculations were performed. For these cross sections, the cross-sectional parameters (L_x, B_p and B_x) and R.W. attachment mode (case 1, 2, and 3) were changed, resulting in a total of 90 cases of calculations. Figure 9 shows the calculation results of the wave overtopping rate considering sea level rise for the "***SMO*** (case 1, 2, and 3)" and the "vertical wall with top heights of hp and $2hp$," respectively. By using ***SMO***, the wave overtopping rate in all cases is less than the tolerable wave overtopping rate up to the S.L.R. +1.1m. The ***SMO*** is smaller than the $2hp$ case up to a S.L.R. +0.5m(+2K). At S.L.R. +1.1m(+4K), however, they are about the same. In Figure 10, the vertical axis is the logarithmic difference between the wave overtopping rate determined for the vertical wall (parapet height: hp) and each ***SMO***, and the horizontal axis is a dimensionless number based on the cross-sectional parameters (L_x, B_p and B_x) and external force parameters (L_0 : wavelength, h_c : crown height and $H_{1/3}$: significant wave height). Based on the relationship between the dimensionless quantities on the vertical and horizontal axes of the graphs, a polynomial approximation is performed for the plots of case 1, 2, and 3, respectively.

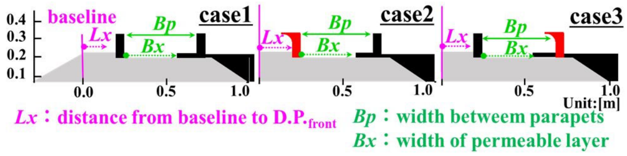

Figure 8 - Cross-sectional shapes of ***SMO***

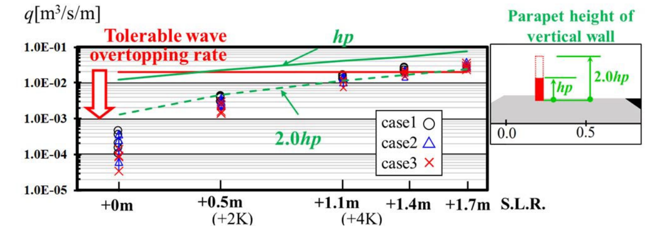

Figure 9 - Relationship of wave overtopping rate of ***SMO*** and sea level rise

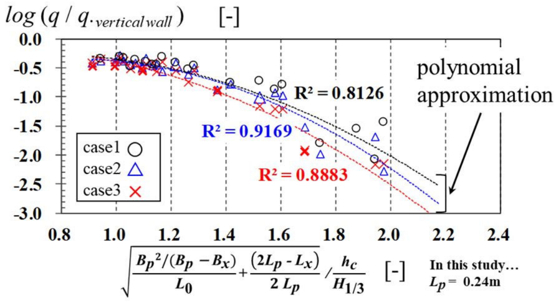

Figure 10 - Wave overtopping rate of ***SMO*** due to cross-sectional parameters

The accuracy of this estimating equation is relatively good, with correlation coefficient(R^2) greater than 0.8 in all cases. From the dimensionless quantities applied to the horizontal axis of the graph, it can be seen that the greater the distance between the parapet(B_p) and the permeable layer (B_x), and the shorter the distance from the reference normal to the D.P.front (L_x), the greater the wave overtopping rate reduction effect. This indicates that the pondng capacity and inundation volume between parapets and the parapet location are dominant in the evaluation of the wave overtopping rate.

CONCLUSION

1) A hydraulic model experiment with sea level rise for an vertical seawall (existing seawall) and ***SMO*** confirmed the effect of ***SMO*** on wave overtopping reduction.
2) P.L. (Permeable Layer) was shown to be the most effective contributor to reducing wave overtopping rate in *SMO*.
3) By using ***SMO***, the tolerable wave overtopping rate was satisfied even under sea level rise (H.H.W.L. +4K scenario).
4) The wave overtopping rate characteristics were clarified using dimensionless quantities with cross-sectional parameters (L_x, B_p and B_x) and external force parameters. For the same cross-sectional parameters, the R.P. (Recurved Parapet) installed at the D.P.rear (Double Parapet) was the most effective in reducing the wave overtopping rate.